Architecture of the Sarcomere Matrix of Skeletal Muscle: Immunoelectron Microscopic Evidence that Suggests a Set of Parallel Inextensible Nebulin Filaments Anchored at the Z Line

Kuan Wang and John Wright

Clayton Foundation Biochemical Institute, Department of Chemistry and Cell Research Institute, University of Texas at Austin, Texas 78712

Abstract. Nebulin, a giant myofibrillar protein (600–800 kD) that is abundant (3%) in the sarcomere of a wide range of skeletal muscles, has been proposed as a component of a cytoskeletal matrix that coexists with actin and myosin filaments within the sarcomere. Immunoblot analysis indicates that although polypeptides of similar size are present in cardiac and smooth muscles at low abundance, those proteins show no immunological cross-reactivity with skeletal muscle nebulin. Gel analysis reveals that nebulins in various skeletal muscles of rabbit belong to at least two classes of size variants.

A monospecific antibody has been used to localize nebulin by immunoelectron microscopy in a mechanically split rabbit psoas muscle fiber preparation. Labeled split fibers exhibit six pairs of stripes of antibody-imparted transverse densities spaced at 0.1–1.0 μm from the Z line within each sarcomere. These epitopes maintain a fixed distance to the Z line irrespective of sarcomere length and do not exhibit the characteristic elastic stretch-response of titin epitopes within the I band domain. It is proposed that nebulin constitutes a set of inextensible filaments attached at one end to the Z line and that nebulin filaments are in parallel, and not in series, with titin filaments. Thus the skeletal muscle sarcomere may have two sets of nonactomyosin filaments: a set of I segment–linked nebulin filaments and a set of A segment–linked titin filaments. This four-filament sarcomere model raises the possibility that nebulin and titin might act as organizing templates and length-determining factors for actin and myosin respectively.

NEBULIN is a giant structural protein that is found in the sarcomere of a wide range of skeletal muscles (8, 11, 20, 23–26, 29). In most vertebrates, nebulin accounts for ~3–4% of total myofibrillar proteins (24, 29), and its size varies from 600 to 800 kD in various muscle tissues (8, 11, 24, 29). Despite its abundance, little is yet known about its molecular structure, morphology, and interactions, since nebulin is difficult to extract in native, intact form from the myofibrillar lattice.

The sarcomere distribution of nebulin has been explored by fluorescent techniques (25, 26, 29). We reported previously that polyclonal antinebulin stained a pair of transverse fluorescent bands that coincide with the phase dense N_2 lines within the I bands of long sarcomeres (>2.5 μm) of glycerinated rabbit skeletal myofibrils (29). Based on the observation that both antinebulin bands and N_2 lines exhibited very similar elastic-stretch dependence on sarcomere length (5, 14), we concluded that nebulin is a component of the N_2 line, which is thought to be attached to longitudinal elastic filaments (9). Furthermore since N_2 lines are frequently found at a point where thin filaments change neighboring relationship and packing geometry (5, 9), it was proposed that nebulin might be involved in the maintenance and regulation of thin filament lattice (23–26).

In the same study (29), however, we noted with concern that in very short sarcomeres (<2.0 μm), the antinebulin staining unexpectedly appeared within the A band and did not stain near the Z line, as would be expected from the reported elastic behavior of N_2 lines (5, 14). Further complexities were evident when detailed dual fluorescence studies of titin and nebulin distribution were undertaken (23, 25, 26). Considerable variations in staining patterns of both titin and nebulin manifested when conventional glycerinated myofibrils were used. Antinebulin would either stain N_2 lines or various loci within A or I bands that were distinct from N_2 lines (25, 26). Occasionally N_2 lines were stained exclusively by antititin instead (23, 25, 26). Furthermore, some long sarcomeres were free of phase dense N_2 lines altogether. We have interpreted such variations as reflecting different degrees of internal damages imparted to the titin/nebulin containing matrix during conventional myofibril preparation, which makes use of a combination of (unsuspected) proteolysis and mechanical shear to achieve segregation of myofibrils (23, 25, 27). Specifically, we proposed that those N_2 lines that are clearly visible as phase dense bands in light microscopy are artifactual and represent loci to which fragmented and damaged titin and/or nebulin translocated and accumulated (25, 26). As a working hypothesis, titin and

nebulin were proposed as components of the same longitudinal filaments, with titin spanning from the M line region across the A band to the N_2 line position near A–I junctions, and with nebulin extending the filament to the Z line (23, 25, 27).

To evaluate this hypothesis, we have performed (*a*) immunoelectron microscopy of mechanically skinned, split muscle fibers that are prepared with minimal proteolysis and little mechanical shear-induced damages; and (*b*) immunofluorescence of myofibrils prepared by an improved procedure that minimizes proteolysis and artifactual N_2 lines (28).

In this paper, we report that such localization studies support the notion that nebulin constitutes a set of long (~1 μm), inextensible parallel filaments attached rigidly to the Z line. Furthermore, since nebulin does not exhibit the characteristic elastic-stretch observed for the I band segment of titin filaments, we conclude that nebulin and titin cannot be serially connected components of the same filament, as previously proposed (23, 25, 27). Instead they are distinct, parallel Z line–linked filaments each with unique molecular characteristics and architectural organization within the sarcomere.

Materials and Methods

Purification and Amino Acid Analysis of Nebulin

Nebulin polypeptide was purified from rabbit back muscle myofibrils by a differential salt fractionation procedure (24) as follows: an SDS solution of rabbit myofibrillar proteins in SDS sample buffer (5 mg/ml in 3% SDS, 10% glycerol, 10 mM Tris-HCl, 1 mM EDTA, 40 mM dithiothreitol (DTT), pH 8.0) was first brought to 0.66 M NaCl and spun at 23,000 *g* for 20 min to remove precipitated titin. The supernatant was then made 0.90 M NaCl to precipitate nebulin. The crude nebulin fraction, redissolved in a small volume of sample buffer and clarified at 23,000 *g* for 20 min, was applied to a 2.5 × 100 cm Sephacryl S500 column equilibrated in 40 mM Tris-Cl, 20 mM sodium acetate, 2 mM EDTA, 0.1 mM DTT, pH 7.5. Fractions were analyzed by 2–12% gradient SDS gels (16) to locate nebulin. Pure nebulin fractions were subjected to amino acid analysis as described (17, 18).

Antibody Production and Immunoblots

Goat antinebulin antibody was prepared against nebulin purified further on a preparative SDS gel, with pulverized gel fragments as the immunogen. The immunoreactivity was established by immunoblot as follows: myofibrillar proteins (~20 μg) were resolved on a 2–12% slab gel and electrophoretically transferred in Towbin's buffer (21) plus 0.05% SDS (31) to nitrocellulose sheets (BA85, 0.2 μm; Schleicher & Schuell, Keene, NH) at 1.6 mA/cm² for 1 h in a homemade semidry transfer unit. A layer of cellulose acetate (ST69, 1.0 μm; Schleicher & Schuell) was placed between the slab gel and nitrocellulose sheet (31) to prevent the soft gel from sticking to the nitrocellulose. The nitrocellulose was blocked with 0.5% (wt/vol) BSA, 0.05% Tween-20, 10 mM Tris-Cl, 0.15 M NaCl, pH 7.5, for 1.5 h at room temperature, incubated with goat antinebulin (1:1,000 dilution) in buffer N (0.1 M KPi, 0.25 M KCl, pH 7.0) for 1.5 h, followed by alkaline phosphatase-conjugated rabbit anti-goat IgG (Miles Scientific Div., Naperville, IL; 1:1,000 dilution in Buffer N) for 1 h. The purple color was developed with BCIP/NBT (Bio-Rad Laboratories, Cambridge, MA). Controls were done either with preimmune serum or by eliminating the first antibody. After photography, the immunostained blot was then stained with india ink to reveal protein patterns. Since background BSA caused only a slight overall staining, a precise matching of immunostaining and protein patterns on the same blot was feasible by this technique.

Gel Analysis of Giant Proteins of Muscle Tissues

Various muscle tissues from the same rabbit or from turkey were quickly removed (10 min postmortem), snap-frozen in liquid nitrogen, and pulverized to fine powders in a mortar under liquid nitrogen. The tissue powders (50 mg) were treated with 2× vol (of tissue weight) of 10 mM DFP in 50% glycerol at −15°C for 2 h and then added with homogenization to 0.2 ml of SDS sample buffer preheated to 95°C in a boiling H_2O bath. The sample was heated for 90 s, cooled to room temperature quickly and then loaded immediately to a long format 2–12% gradient gel (model SE280; Hoefer Scientific Instruments, San Francisco, CA; 8 × 10 cm). Electrophoresis was carried out at 30 mA for 2.5 h.

Split Muscle Fiber Preparation and Antibody Labeling

The technique is described below and in diagrammatic form in Fig. 4. New Zealand white rabbits (2–3 kg) were anesthetized with an intramuscular injection of 2.5 ml 90% ketamine (Bristol BVP 100 mg/ml)/10% acepromazine and bled just before dissection. Psoas was exposed through a lateral incision and irrigated with ~10 ml of a relaxing buffer plus protease inhibitors (150 mM K propionate, 5 mM KH_2PO_4, 3 mM Mg acetate, 5 mM K·EGTA, 5 mM NaN_3, 20 μg/ml leupeptin, 5 μg/ml aprotinin, 1 mM DTT, 3 mM ATP, pH 7.0) held at 0°C. Small bundles of tissue (~2–3 mm in diameter, 10–15 mm in length) were removed with care to avoid any stretching of the fibers, and then transferred through a relaxing buffer wash at 0°C and placed in a Petri plate containing a Sylgard dissection base (model 182 elastomer; Dow Corning Corp., Midland, MI) and relaxing solution. The tissue bundles were allowed to set in the relaxing solution at 0°C for 2 h before mechanical skinning to facilitate adequate infiltration of the relaxing buffer and protease inhibitors. With the aid of Dumont No. 5 tweezers, single fibers were isolated from the tissue bundles under a dissection microscope and pinned at one end by insertion into the dissection base. Once pinned, the fiber was "skinned" by grasping a few myofibrils, teased away at the free end of the fiber, and pulling them slightly up and away from the remaining myofibrils held at rest length. The sarcolemma was rolled up by the separating myofibrils. The larger myofibril bundle denuded of its sarcolemma were separated into two to four equal-diameter split fibers with a minimum of stretching and were affixed temporarily by pressing the ends into the Sylgard.

Gold slot grids (model GS2X1; Polysciences, Inc., Warrington, PA) that had previously been scored on the edges were now placed alongside the split fibers in the Petri plate, and with tweezers the split fibers were grasped, stretched slowly in small increments to the appropriate sarcomere length (generally 100, 150, and 200% of rest length), and affixed to the rough edges on the slot grid. Typically, two marks were scored at one end of the slot to aid in identifying split fibers of differing sarcomere length. After three fibers of varying sarcomere lengths were mounted on one grid, it was removed from the Petri plate, transferred to a freshly prepared formaldehyde/PBS fixative (3.7% paraformaldehyde, 2.7 mM KCl, 1.5 mM KH_2PO_4, 137 mM NaCl, 8 mM Na_2HPO_4, pH 7.2) for 10 min and washed for 10 min (two changes) in PBS, followed by blocking for 20 min at 4°C in PBS/1% BSA. Split fibers so mounted were easily transferred from one solution to another without undue stress from surface tension because they were surrounded by a droplet of solution on the slot grid.

Grids with mounted split fibers were placed in primary antibody solution (50 μg/ml goat antinebulin IgG in PBS/BSA) in a Terasaki microtiter plate with V-shaped 10-μl wells that was well-sealed with parafilm to prevent drying and incubated in a humid chamber at 4°C for 1 h. Primary antibody was washed away for 30 min (five changes) in PBS/BSA. The grids were treated with secondary antibody (50 μg/ml rabbit anti-goat IgG (H&L) (Capell Laboratories, Malverne, PA) for 6 h at 4°C, followed by a 30-min wash (five changes) in PBS/BSA. The grids were transferred to a solution of protein A–colloidal gold conjugate (3–5 nm in diameter, prepared by phosphorus reduction according to DeMey (4) with absorption maximum at 512 nm, A_{512} = 0.25) for 15 h at 4°C, followed by a 15-min (two changes) PBS/BSA wash and a 30-min (five changes) PBS wash.

Electron Microscopy

All grids with split fibers were transferred to beem capsules (size 00; Polysciences, Inc.), fixed in 2% glutaraldehyde, 0.05 M Na cacodylate, pH 7.4, at 4°C for 35 min, washed in H_2O, and dehydrated by a graded series of dimethylformamide. The grids were embedded en bloc in the capsules by UV-polymerization in Lowicryl K4M at 4°C (modified from Altman et al. [1]). The embedded fibers on the grid were sectioned with the knife edge parallel to the fiber axis to avoid distortion in the longitudinal dimension. The soft gold grid served as a visual marker to guide trimming and knife advance but did not interfere with sectioning. Sections were stained with 0.5% aqueous uranyl acetate and Reynold's lead citrate and photographed on a JEOL-100CX electron microscope. Micrograph magnification was calibrated with a carbon grating standard (No. 1602; Ernest F. Fullam, Inc., Schenectady, NY).

Measurements of point-to-point distances along the long axis of the sarcomere were made on prints (Kodabrome II RC paper) with a Sigma Scan Digital Measurement System (Jandel Scientific, Sausalito, CA), including sarcomere length, I filament length, A band width, and six antibody stripes or gold clusters to Z line distances (Na to Nf.) Data from ~100 sarcomeres were transcribed into Multiplan spreadsheet (Microsoft, Seattle, WA), and all values were normalized with their respective I filament lengths set to 1.13 μm (center of Z line to distal end of the thin filament) before plotting.

Immunofluorescence Microscopy

Rabbit psoas myofibrils were prepared with a Triton/EDTA procedure of Wang and Ramirez-Mitchell (28). Immunofluorescence of antinebulin was done on either unfixed or formaldehyde-fixed myofibrils that were settled and adhered to glass coverslips, as described previously (29). Antinebulin was applied as purified IgG fraction (10–50 μg/ml) pretreated with 0.5 mM PMSF, 5 mM DFP to minimize proteolysis during incubation. Extractions of myofibrils with high salt buffers were done by irrigating from one side of the sample slide with either A band solvent (0.6 M KCl, 2 mM $MgCl_2$, 2 mM EDTA, 2 mM NaPPi, 0.1 mM DTT, pH 6.8) or A plus I band solvent (0.6 M KI, 0.1 M Tris-Cl, 3 mM EGTA, 50 mM $Na_2S_2O_3$, 0.1 mM DTT, pH 7.5) and withdrawn from the other side with a wedge of filter paper. The degree of extraction is varied by substituting the solvents with PBS at various times. All extracted myofibrils were fixed with formaldehyde before antibody staining. A Zeiss IM 35 photomicroscope with epifluorescence attachment was used for photomicroscopy.

Results

Nebulin Purification and Characterization

Nebulin polypeptide from rabbit skeletal muscle was purified by an extension of a novel salt fractionation procedure that was originally developed for titin preparation (24; Fig. 1, *a–c*). Based on an observation that most SDS-solubilized myofibrillar proteins, exclusive of nucleic acids, will precipitate roughly in the decreasing order of polypeptide sizes, when NaCl concentration was raised beyond 0.6 M (18, 24), nebulin was first enriched 7–10-fold by precipitation between 0.66 and 0.9 M (Fig. 1, *a* and *b*). After further size fractionation on a Sephacryl S500 gel filtration column (Fig. 1 *c*), pure nebulin, free of contaminating nucleic acid, titin, and myosin heavy chain was obtained in high yield (2 mg/100 mg of myofibrillar protein).

Its amino acid composition (Table I) is distinct from titin, especially in the lower proline content (5.9 vs. 7.4% in titin), and a higher total content of lysine, arginine, asx, and glx (41.1 vs. 33.9% in titin; 26). Rabbit nebulin, however, is very similar in composition to nebulins purified from frog gastrocnemius (17) and mouse diaphragm muscles (18).

Antinebulin antiserum reacted specifically with a single nebulin band on blots of rabbit myofibrillar proteins, with no evidence of cross-reactivity with titin (see Fig. 3). The specificity of antinebulin was consistently demonstrated on immunoblots only after a modified buffer, Buffer N, was developed. For reasons still unclear, many (>80%) of commercial enzyme-conjugated secondary antibodies that we used exhibited a tendency to bind directly and selectively to nebulin bands on the nitrocellulose blot, thus giving a false positive band in control samples stained with preimmune or with no primary antibodies (data not shown). No binding was observed with either unconjugated peroxidase or alkaline phosphatase (not shown). This nonimmunological interaction was eliminated by the high ionic strength buffer, suggesting an ionic origin. It should be noted that such interaction appears to be limited to nebulin blotted from SDS gels, since no labeling of native nebulin in the sarcomere could be detected when the sarcomeres were stained with preimmune antibody followed by either fluorescent second antibody or colloidal gold conjugates (see localization studies below).

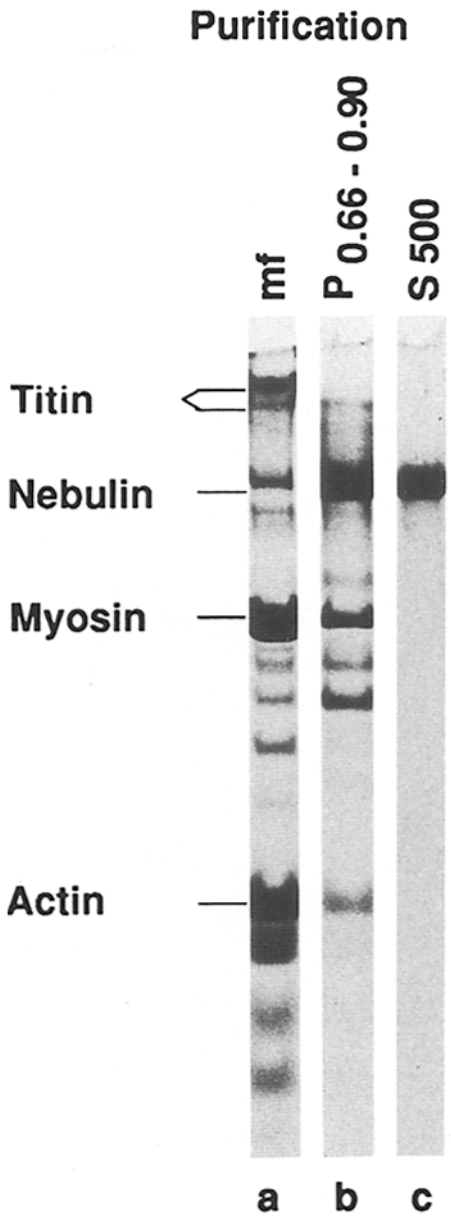

Figure 1. Purification of rabbit nebulin. Nebulin was purified from rabbit back muscle myofibrillar proteins (*mf*) that were solubilized in SDS (lane *a*), salt fractionated by precipitating crude nebulin between 0.66 and 0.90 M NaCl ($P_{0.66\text{-}0.90}$; lane *b*), and size fractionated on a Sephacryl S500 column to yield pure nebulin (lane *c*). Gel electrophoresis was done on a 2–12% gradient gel.

Giant Titin-sized and Nebulin-like Proteins in Muscle Tissues

The wide spread distribution of giant polypeptides of the size of titin and nebulin was first suggested by gel analysis of purified myofibrils (29) or whole tissues (8, 11) in a wide range of vertebrate and invertebrate species. However, whether these proteins are related chemically or immuno-

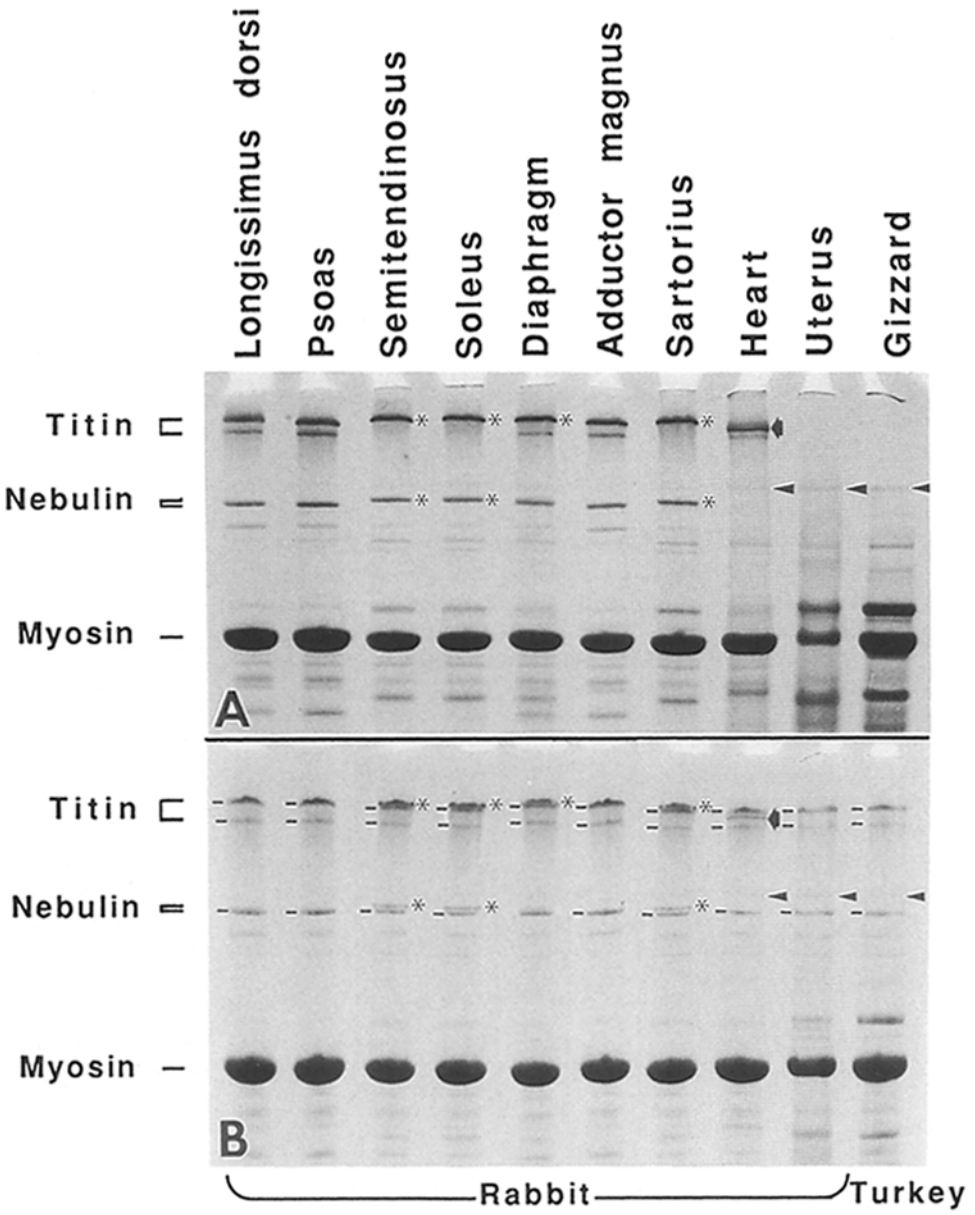

Figure 2. Giant proteins in skeletal, cardiac, and smooth muscle tissues. Muscle tissues were snap frozen, pulverized in liquid nitrogen, solubilized in hot SDS solutions, and analyzed on a 2–12% gradient polyacrylamide gel (*A*). To reveal subtle mobility differences, psoas muscle sample was added to each muscle as an internal standard and the mixtures were subjected to electrophoresis in *B*. Only the top portion of each Coomassie Blue–stained gel pattern is shown. Titin and nebulin bands marked by asterisks are appreciably larger than the psoas proteins. Note that cardiac muscles have smaller titins (marked by *black arrow*) and no detectable nebulin. Protein bands labeled by arrowheads in cardiac and smooth muscles (*uterus* and *gizzard*) are significantly larger than nebulin.

chemically to skeletal muscle nebulin remained, with one exception, unexplored (20). We have examined the gel patterns of several fast and slow skeletal muscles, cardiac muscle from rabbit, and smooth muscles from rabbit and turkey by directly solubilizing snap-frozen tissue powders in hot SDS to minimize degradation of giant proteins (see Materials and Methods). As shown in Fig. 2 *A*, all skeletal muscles tested contained significant amounts of titin/nebulin-sized proteins. It is interesting that there is a small yet significant mobility difference among proteins within each family. This was revealed clearly when a mixture of two muscle tissues were subjected to electrophoresis (Fig. 2 *B*). Nebulin in these muscles fall roughly into two size groups: semitendinosus, soleus, diaphragm, sartorius > adductor magnus, longissimus dorsi, psoas (Fig. 2 *B*). These two groups of size variants may differ up to 10–15% in mass and were not artifacts resulting from sample preparation since there was no evidence of partial interconversion or formation of multiple bands whenever protocols are strictly adhered to. Immunoblots with antinebulin indicated strong cross-reactivity amongst members of nebulin family, with no cross-reactivity with titin (Fig. 3).

In rabbit cardiac muscle tissue, only one minor band was present in the nebulin region (*arrowheads*, Fig. 2 *A*). This and other trace components in this region contributed ~0.2% of total proteins and thus were an order of magnitude lower in abundance than skeletal nebulin. It is interesting that similar bands were also found in rabbit uterus and turkey gizzard smooth muscles, especially in overloaded gels (Fig. 2 *A*). The identity of these minor bands, which are larger than skeletal muscle nebulin, remained uncertain. So far, no cross-reactivity of these proteins with antiskeletal muscle nebulin could be demonstrated on immunoblots (Fig. 3).

Preparation of Split Muscle Fibers for Immunoelectron Microscopy

Split muscle fiber preparations, consisting of bundles of roughly 20–300 myofibrils have been developed to achieve

Table I. Amino Acid Compositions of Nebulin and Titin

Amino acid (mol %)	Rabbit*		Frog‡		Mouse§		Chicken‖	
	Nebulin	Titin	Nebulin	Titin	Nebulin	Titin	Nebulin	Titin
Asx	12.1	9.6	11.0	8.7	12.5	9.4	11.1	9.3
Thr	5.5	7.9	5.4	6.7	5.4	8.7	7.0	6.6
Ser	7.5	7.4	5.5	6.4	7.1	7.4	6.2	6.7
Glx	13.6	13.7	14.0	13.3	9.0	8.0	12.8	11.8
Pro	5.9	7.4	4.5	8.8	4.5	6.5	3.0	6.7
Gly	5.5	6.5	4.3	7.2	5.1	6.2	5.2	7.6
Ala	7.6	6.6	7.9	7.3	7.0	5.9	7.6	7.5
Cys	0.6	0.8	0.4	0.5	0.7	1.0	0.8	0.6
Val	4.8	7.4	6.4	11.0	6.8	10.0	8.2	7.8
Met	1.5	0.8	1.9	1.1	3.0	1.6	0.7	1.6
Ile	3.3	4.4	5.0	6.4	5.7	6.7	6.1	5.6
Leu	6.8	6.5	8.1	7.2	8.6	7.6	7.9	7.6
Tyr	4.1	2.8	4.5	3.5	3.7	2.5	1.5	3.0
Phe	2.3	2.4	2.3	3.0	2.4	3.0	2.7	2.9
Trp	ND	ND	ND	ND	ND	ND	ND	ND
Lys	11.3	10.2	10.6	8.4	11.6	9.3	11.1	7.9
His	3.3	1.7	3.4	1.8	2.7	1.5	2.8	1.8
Arg	4.1	4.4	4.6	5.6	4.2	4.6	5.4	5.0

* This work.
‡ From Somerville and Wang (17).
§ From Somerville and Wang (18).
‖ From Maruyama et al. (12).

consistent and reproducible antibody labeling patterns at electron microscopic resolution (see Fig. 5). Since muscle fibers were processed promptly postmortem in the presence of protease inhibitors, no proteolysis of titin and nebulin was evident from gel analysis (data not shown); furthermore, since the preparation has not been subjected to conditions that promote rigor bridge formation between thick and thin filaments, these myofibrillar bundles could be stretched in a relaxing buffer to sarcomere lengths well beyond nonoverlap without tearing the sarcomere and producing excessive loss of striations and lateral alignment. The detection and quantitation of antibody density are thus facilitated. Equally important, by removing sarcolemma and reducing the fiber diameter, problems with antibody accessibility that generally plague whole tissue labeling, were effectively resolved. This is illustrated by the uniform labeling of all sarcomeres in the low magnification survey section (Fig. 5). Our earlier attempts of labeling muscle fiber bundles or single fibers permeabilized by Triton X-100 or EGTA yielded, at best, fibers labeled only at the superficial layer of myofibrils. Gold conjugates frequently failed to penetrate and were found entrapped in the leaky sarcolemma layer (our unpublished observations). An additional advantage of split fiber preparations is that their active and passive mechanical properties can be measured directly with sensitive force transducers, thus facilitating correlative studies of sarcomere structure and function.

An obvious trade off of such preparations is that they are prone to breakage when subjected to handling, especially during infiltration and embedding in viscous plastic solution. Furthermore, the entire fiber may be lost with one misplaced cut during sectioning of plastic embedded fibers. The use of single-slot grids as fiber holders throughout the entire sequence of steps (Fig. 4) obviates some of these technical problems: fiber breakage is minimal and the embedded grid serves as a visual marker for sectioning. Further, the grids made it feasible to process multiple fibers at different sarcomere lengths under identical conditions throughout the various steps of immunoelectron microscopy. Many potential interpretation problems of comparing individually prepared samples are thus avoided altogether.

Distribution and Stretch Behavior of Nebulin Epitopes

As indicated in the low magnification survey of antinebulin-labeled split fiber (Fig. 5) all sarcomeres within the myofibrillar bundle were uniformly labeled by antibodies to give rise to, in this instance, two transverse stripes within the I band (*solid arrows*, Fig. 5). That these stripes indeed resulted from specific antibody binding to nebulin epitopes is demonstrated by the following. (*a*) These stripes were absent in unlabeled controls, in preimmune controls (*open arrows*, Fig. 5, *inset*), and in controls eliminating one or two antibodies. (*b*) These stripes were specifically labeled by protein A–gold conjugates. Presumably due to pronounced steric hindrance, gold conjugates exhibited a gradient of labeling density, which decreases toward the interior of the split fiber (Figs. 5, 6, *A* and *C*). It was noted that sarcomeres in the surface-bound myofibrils frequently were not as well-preserved as the interior ones. Such "open" sarcomeres appear to be more accessible to gold conjugates (Fig. 6, *B* and *C*).

The distribution and stretch behavior of nebulin epitopes were investigated using split fibers, with sarcomere lengths ranging from resting length (2.3 μm) to well over nonoverlap (4.5 μm; Fig. 7).

In highly stretched fibers where A segments and I segments were pulled away from each other, exposing the slender titin filaments (*T* in Fig. 7, *A* and *B*) bridging the gaps in these nonoverlap sarcomeres, a total of five to six antibody stripes, located from 0.1 to 1.0 μm from the center of the Z line (designated as *a–f*) were present in each side of those I segments that still retained sufficient lateral registry (Fig.

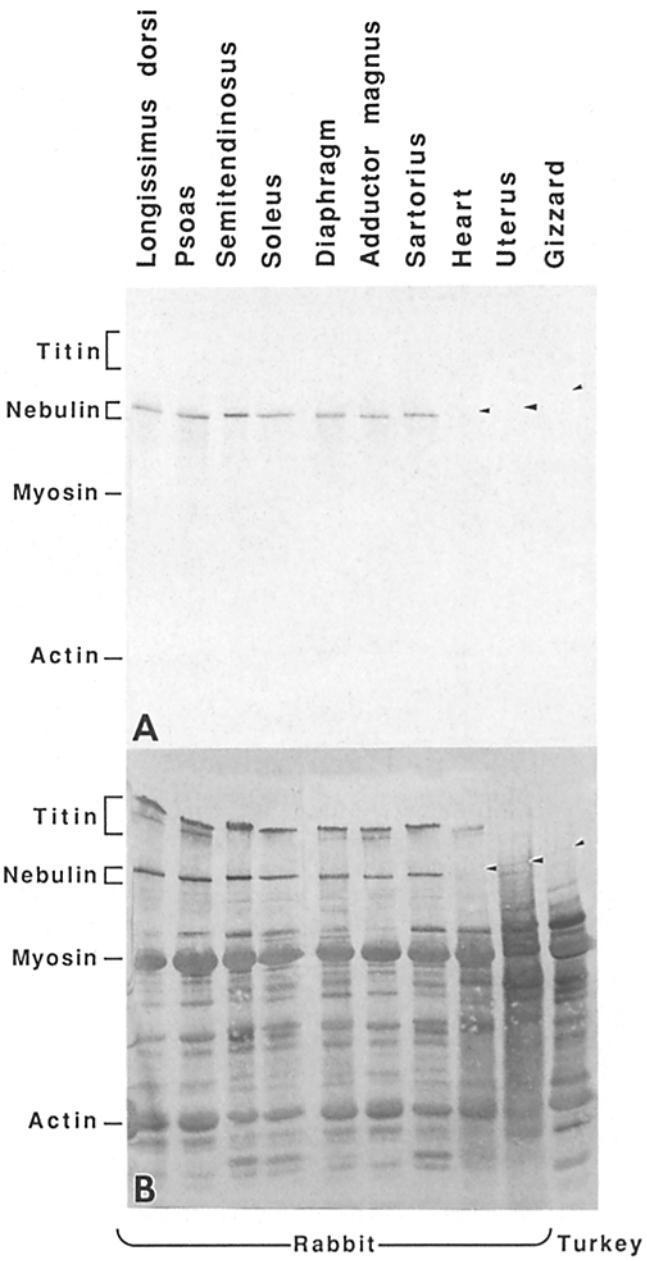

Figure 3. Western analysis of cross-immunoactivity of nebulins. Muscle samples prepared as in Fig. 2 were subjected to electrophoresis, transferred to a nitrocellulose sheet, and stained with goat antinebulin. Alkaline phosphatase-conjugated secondary antibody was used to detect binding (*A*). After color development, the sheet was stained with india ink to reveal protein patterns (*B*). Note the absence of antinebulin in cardiac, uterus, and gizzard smooth muscles (*arrowheads*).

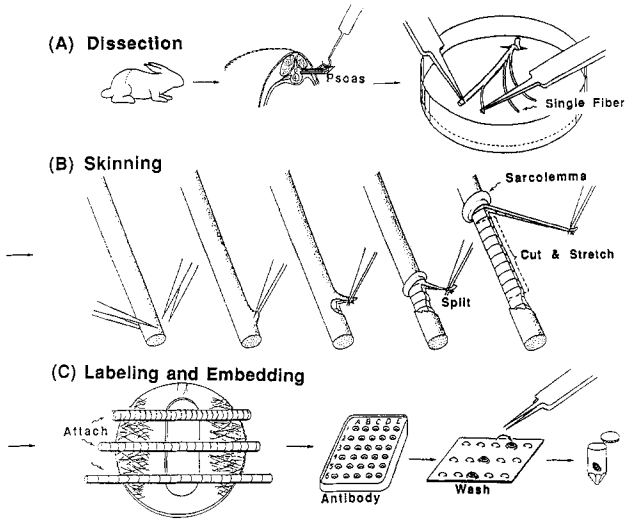

Figure 4. Preparation of split muscle fibers for immunoelectron microscopy. This schematic diagram illustrates essential steps described in detail in Materials and Methods.

7 *B*). Due to the substantial stress (resting tension) at this sarcomere length, many sarcomeres are distorted to such an extent that antibody stripes were smeared together and recognized only by the presence of gold beads (data not shown). A small number of gold beads were occasionally seen in the gap region (Fig. 7 *B*, *left*). Since such labeling only occurred at the distal ends of distorted and misaligned I segments and that such scattered labeling never aligned transversely to indicate regularity, we conclude that these gold beads were labeling translocated nebulin epitopes that originated from loci near the edge of the I band. As expected, neither antibody stripes nor gold particles were observed in control samples (Fig. 7 *A*).

In split fibers with decreasing sarcomere lengths where thick and thin filaments begin to overlap, the number of antibody stripes decreased gradually from six to only one in resting length sarcomeres (2.3 μm). Closer examinations of the banding patterns (Fig. 7) suggested that the "missing" antibody stripes distal to the Z line may have entered the A band and were obscured by the dense structure. This conclusion is supported by the following observations. (*a*) In grazing sections of A bands, gold clusters were seen aligned transversely into stripes at the expected axial position of missing stripes (Fig. 7, *D* and *E*). These gold stripes most likely resulted from the labeling of more accessible nebulin epitopes near the very surface of the A band. (*b*) In longitudinal sections of A bands, clusters of gold beads were frequently found at the perimeter of A bands at axial positions that correspond to the distal antibody stripes (Fig. 7 *E*). Such peripheral gold clusters appear to be "cross-sectioned" gold stripes that have labeled the A band surface. Occasionally some gold clusters were seen located at some distance from the sarcomere surface (e.g., Fig. 7 *E*), presumably resulting from labeling of dangling nebulin filaments away from the surface.

To quantitate the stretch response of nebulin epitopes, the spacing from the center of each stripe to the center of Z line was measured, using either antibody density, gold stripes, or gold clusters as markers of axial positions. The identification of each stripe was further aided by the observation that the relative intensity and relative width remained unchanged at different sarcomere lengths, with Nb, Nc>Nd, Ne>Nf>Na. There was thus no evidence of any epitope cross-over or inversion that would confuse identification.

It should be noted that Na, the stripe closest to the Z line, was a great deal weaker and more diffuse than the rest and was identified unambiguously only by gold labeling (Fig. 7 *F*). Since it is not uncommon to observe diffuse density near

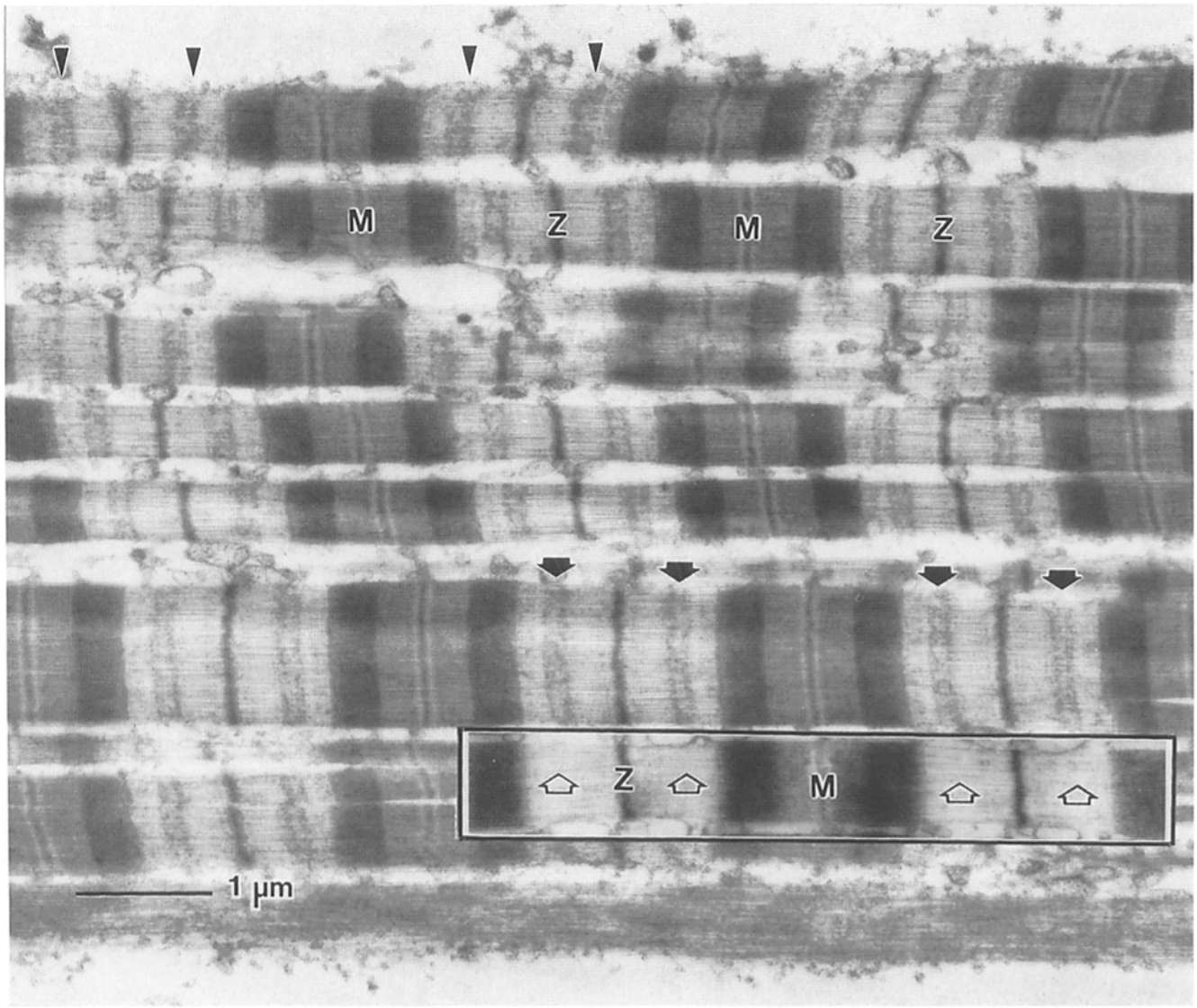

Figure 5. Nebulin localization in rabbit psoas split fibers. A low magnification survey of antinebulin-labeled rabbit psoas split fiber at 2.8 μm sarcomere length, as described in Materials and Methods. Note the uniform penetration of antibodies into the interior sarcomeres to give rise to, at this length, two dense stripes within each I band (*solid arrows*). Such antibody-imparted stripes are absent in preimmune controls (*open arrows*, *inset*). Protein A–gold conjugates, used to confirm antibody labeling, are consistently observed coinciding with the antibody density only in the superficial layers of myofibrils (*arrowheads*) but are absent in the interior ones (*solid arrows* near the center).

the Na position in unlabeled control sarcomeres (not shown), we have included for quantitative analysis, only those Na stripes with clear evidence of gold labeling. We have also noticed that in a few cases, where the 40-nm repeat of the I band was visible, Nb and Nc stripes were seen as fine granular densities that accentuated, for Nb, the 7th (weak), 8th and 9th (strong) repeat, and, for Nc, the 10th (weak), 11th and 12th (strong) repeat (Fig. 7 *D*), giving the impression that the accessible nebulin epitopes may be related by a 40-nm repeat.

A plot of antibody spacings vs. sarcomere length (Fig. 8) clearly indicated that, within experimental errors, the axial spacing of each stripe remains constant throughout the range from 2.3 to 4.5 μm. Thus nebulin epitopes exhibited none of the pronounced elastic stretch dependence shown by the I band segment of titin filaments (30), nor the elastic stretch-response of N_2 lines (5, 14).

Immunofluorescent Localization of Nebulin in Isolated Myofibrils

Immunofluorescent localization of nebulin was carried out on myofibrils that were prepared with minimal proteolysis and lattice distortion as evidenced by the lack of phase-dense N_2 lines in long sarcomeres (28). As shown in Fig. 9 *A*, for sarcomeres of moderate length (~2.8 μm), the fluorescent staining patterns consisted of a pair of prominent wide bands in the I band (designated as α in Fig. 9), a pair of dim and broad zones coinciding with the overlap region of the A band (designated as β in Fig. 9 *A*), and a narrow band at the Z line

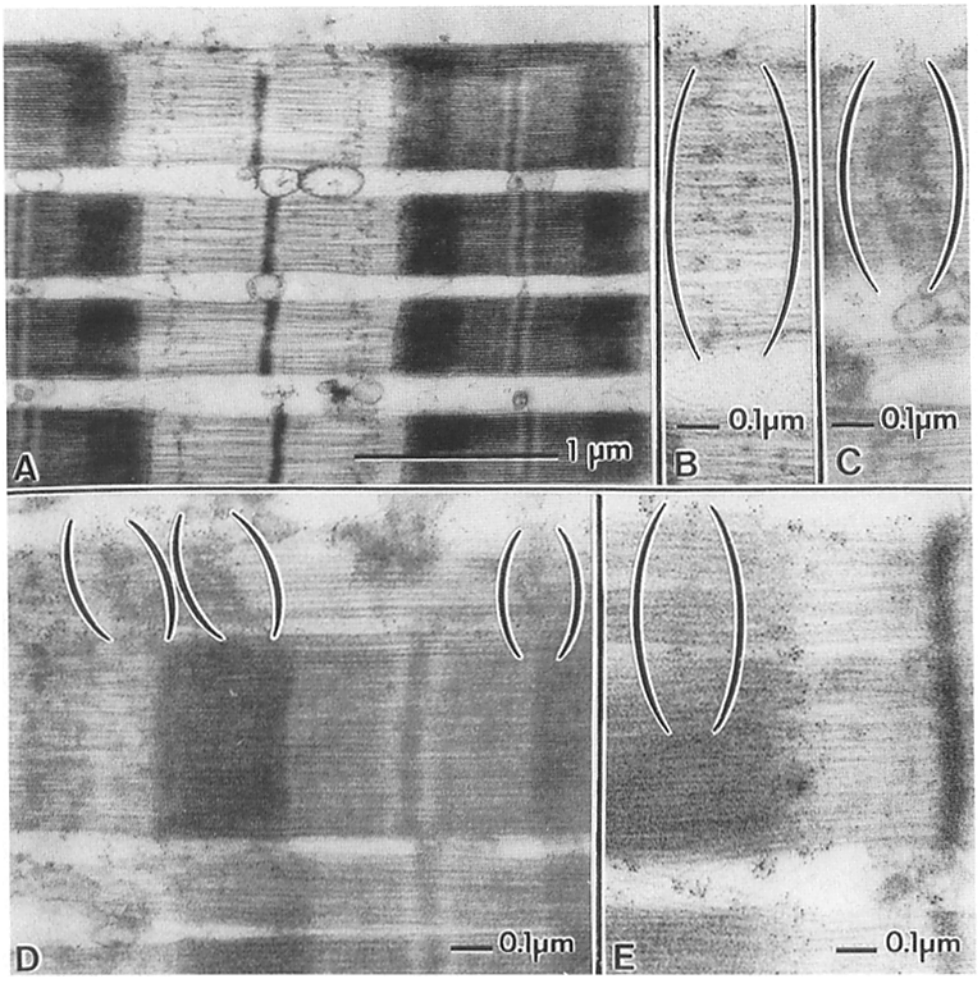

Figure 6. Antibody density and gold conjugates as complementary markers of nebulin epitopes in the I and A bands. Nebulin epitopes are identified by antibody density or by gold labeling. The sparse antibody-imparted densities coincide with all gold beads (*brackets*). The 3–5-nm gold beads, however, frequently fail to penetrate more than a few layers of myofibrils and, as illustrated in *C*, label only the outermost sarcomere near the top (*bracket*) but not the one immediately below. Gold beads are instrumental in identifying additional epitopes within the A band where antibody density is difficult to detect. In grazing sections, *D* and *E*, gold beads are seen aligned into broad stripes on the surface of the A band (*brackets*).

position. The β zone staining, being much dimmer than the adjacent α bands, was photographed clearly only under conditions that overexposed α bands, causing in some cases the merging of α bands with Z line staining (cf. Fig. 9 *B*). A comparison with an electron micrograph at comparable sarcomere length (Fig. 9 *A*) indicated that, at this length, the α bands correspond to Nb and Nc staining, the β zones to Nd, Ne, and Nf staining, and the Z staining to Na's. The dim staining of β zone suggested that the steric hindrance of nebulin labeling exerted by A band components as observed in immunoelectron microscopy is also evident in immunofluorescence.

As sarcomere length decreased, staining patterns underwent a series of transitions that are best illustrated by myofibrils that exhibited a graded change in sarcomere length from one end (3.0 μm) to the other (2.0 μm) (left to right in Fig. 9 *B*): the α bands and Z staining transformed gradually into one dim narrow line near the Z line, whereas β zones merged into a bright sharper line in the center of the A band. In even shorter sarcomeres (<2.0 μm) where double overlap of thin filaments across the bare zone occurred, two dim fluorescent bands coincided with the phase dense doublet near the center of the sarcomere (Fig. 9 *C*). The narrowing and fading of α bands in shorter sarcomeres (Fig. 9 *B*) may result from the gradual entrance of Nb, Nc, and Na epitopes into the A band, becoming less accessible to antibody. Similarly, the merging and brightening of β zones in the mid-A position may be caused by the appearance of Nf, Ne, Nd epitopes in the more accessible central bare zone of the A band. The doublet staining of double overlap sarcomeres (Fig. 9 *C*) suggests that Nf, Ne, Nd epitopes may have moved across and reached to the other side of the bare zone (as thin filaments did) and were somewhat accessible to antibodies because of the expanded interfilament spacings in extremely short sarcomeres.

The fluorescent staining of intact sarcomeres are thus consistent with the immunoelectron microscopic results in revealing the inextensible nature of nebulin and the sliding of nebulin epitopes into the A band as sarcomeres shorten. The fluorescence data further demonstrate that in very short sarcomeres, from which immunoelectron microscopic data are lacking, nebulin still maintains the same inextensible characteristics, resulting in a "double overlap" pattern similar to that of thin filaments.

Additional studies were carried out with myofibrils that were selectively extracted with high salt solutions. Staining patterns of myofibrils that have been extracted with either 0.6 M KCl to remove A bands (Fig. 9, *D–F*) or with 0.6 M KI

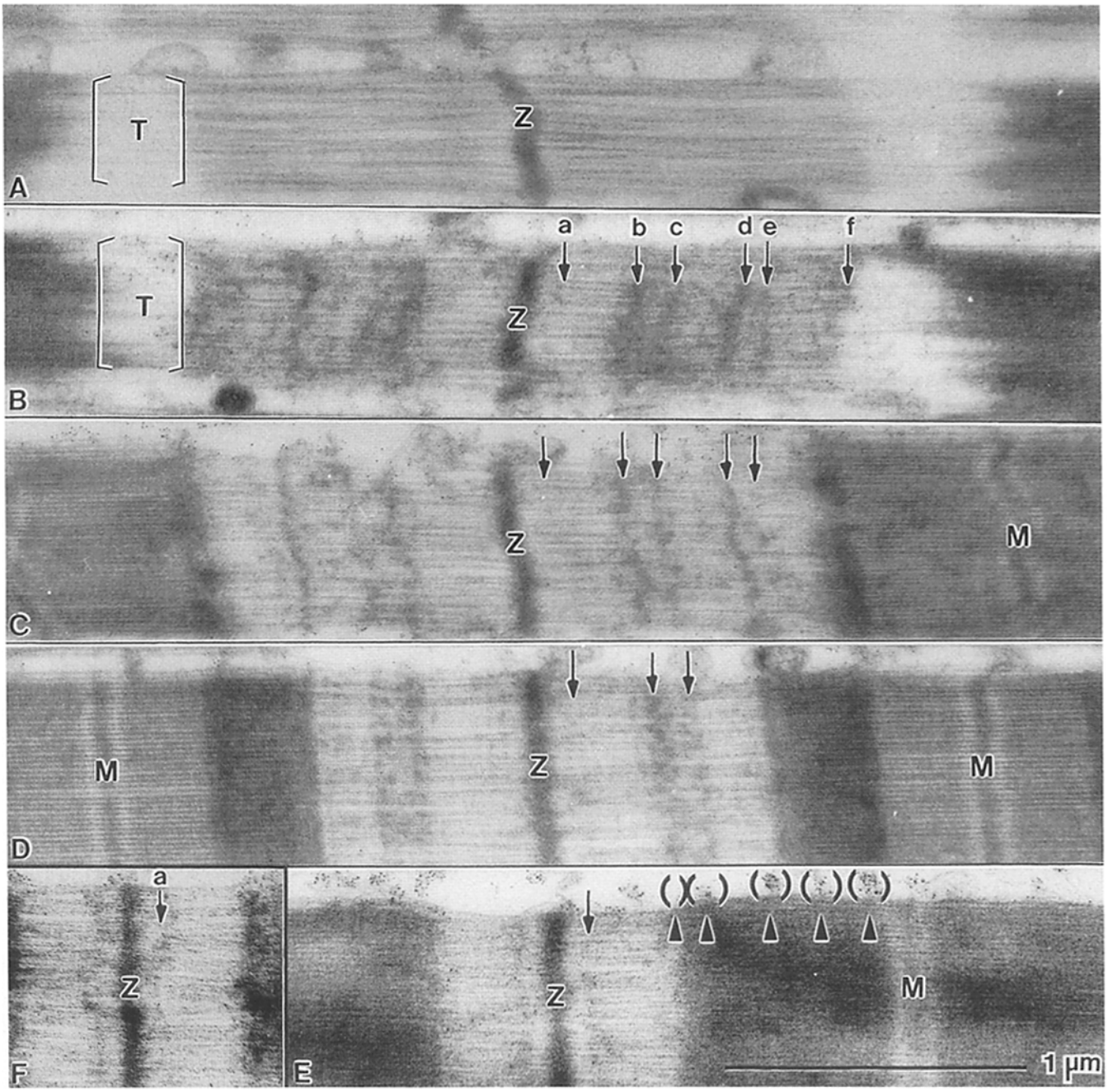

Figure 7. Distribution and stretch response of nebulin epitopes. Rabbit psoas–split fibers were stretched to various sarcomere lengths and labeled with antinebulin and protein A–gold conjugates as described in Materials and Methods. A preimmune control of nonoverlap sarcomeres in *A* indicates the absence of prominent I band striations as opposed to those present in antinebulin-labeled sarcomeres displayed in decreasing lengths from *B* to *F*. *T* in *A* and *B* indicate titin filaments spanning the gaps of disengaged A and I segments in such sarcomeres. Antibody stripes in the I band are designated *a–f* (*arrows*) and the axial position of the distal epitopes that have entered the A band are detectable by gold clusters (*brackets*) indicated by arrowheads in *E*. Gold labeling of the stripe *a* is indicated by an arrow in *F*.

solution to remove A and I bands (Fig. 9 *H*) suggested that, as is the case with titin (26, 27, 28), translocation of epitopes has occurred to various degrees after extractions. For 0.6 M KCl extraction, this was demonstrated by myofibrils that exhibited a graded degree of extraction of A bands from only one end (Fig. 9 *D*, empty circles at right), obtained by interrupting extraction during irrigation: a gradual narrowing of the normal α bands–Z staining triplet into a brighter doublet occurred as the degree of extraction increased toward the right side of the myofibril. Such transitional patterns were also observed separately in individual myofibrils with uniformly extracted sarcomeres (Fig. 9, *E–G*). It is significant that the width of the doublet was either the same or narrower than the phase images of the remaining I segments, suggesting a partial translocation of nebulin toward the Z line that is unaccompanied by thin filaments. In KI-extracted resi-

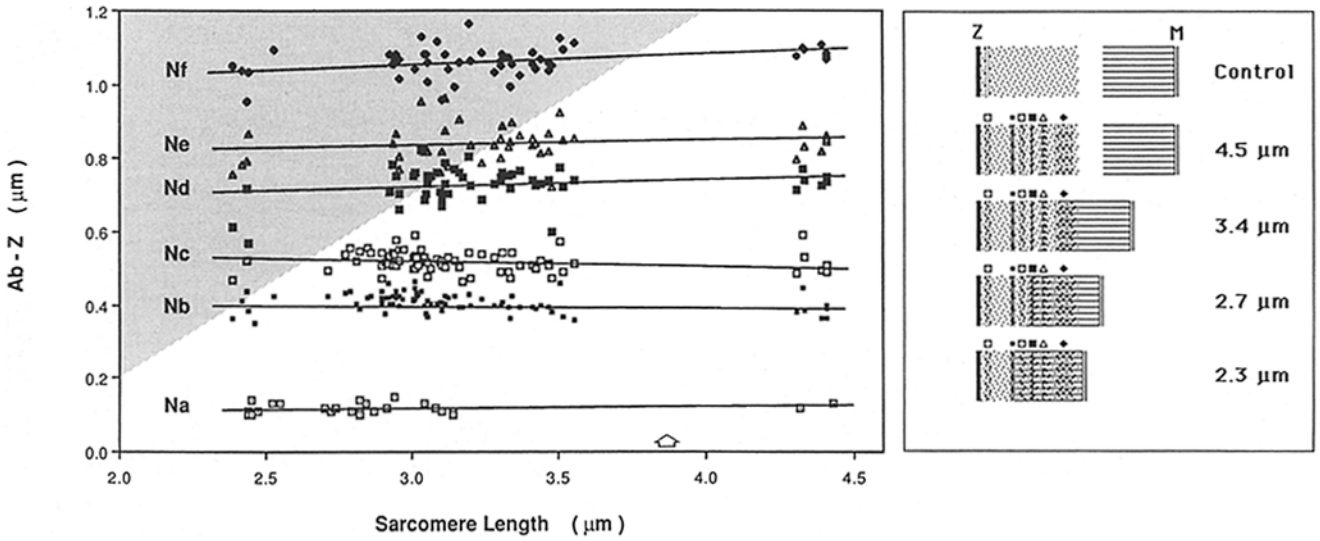

Figure 8. Quantitation of stretch response of nebulin epitopes. Antibody spacings, the center-to-center distance between each stripe and the Z line, are plotted as a function of sarcomere length. The shaded area indicates data points that were collected using peripheral gold clusters or gold stripes in grazing sections as markers of A band epitopes. A schematic diagram is presented on the right. Nebulin epitopes span at least 1 μm with no evidence of stretch-sensitivity over a wide range of sarcomere lengths from resting length (2.3 μm) to beyond overlap (4.5 μm). The arrow near 3.9 μm indicates the sarcomere length at which myosin and actin filaments begin to disengage.

dues, which consisted mainly of translocated titin and nebulin (28), antinebulin intensely stained the KI-doublet (Fig. 9 *H*). These data suggest that the 0.6 M KCl treatment not only extracted A band, but also uncoupled, at least partially, the synchronous sliding of nebulin and actin in intact sarcomeres. Treatment with 0.6 M KI, which removed the majority of actin and myosin (Fig. 6 of reference 28), caused the uncoupled nebulin to retract toward the Z line position, suggesting a stable structural linkage of nebulin to the Z line.

Discussion

Nebulin: A Family of Giant Structural Proteins

The data presented here supported our previous conclusions that nebulin represents a family of giant structural proteins (600–800 kD) that are major components (~3% of total myofibrillar proteins) of skeletal muscle sarcomeres (23–26, 29). Within the nebulin family, immunological cross-reactivity among skeletal muscles of rabbits as well as across species (e.g., human [20], chicken, dog, mouse, and baboon [unpublished data]) suggests some sequence homology. Indeed, the amino acid compositions of several purified nebulin (rabbit back muscle [this work], frog gastrocnemius [17], and mouse diaphragm [18]) are very similar. It is noted that nebulin in various skeletal muscle tissues from rabbit are not identical in size. These size variants might represent tissue-specific isoforms, since there was no evidence of proteolysis-induced interconversion of these forms.

Is Nebulin Absent in Cardiac and Smooth Muscles?

In our preliminary gel analysis of glycerinated chicken and rabbit cardiac myofibrils, a large major nebulin-sized protein was found in these samples (quoted in reference 29). Subsequent Western blot analysis indicated that it is a large proteolytic fragment of cardiac titin and, with improvements in sample preparative procedure that minimizes proteolysis, this major band is no longer observed (unpublished data). In intact cardiac muscle tissues, proteins of low abundance (<0.2%) similar in size to nebulin are detectable in patterns of overloaded gels (Fig. 2). So far, no cross-reactivity of these proteins with antiskeletal nebulin could be demonstrated on immunoblots. Supporting this negative result is our recent demonstration that no nebulin message RNA was found in human cardiac muscles by Northern analysis with a cDNA probe to human nebulin (20). Taken together, the data suggest that the nebulin gene, at least the skeletal muscle type, is not expressed in cardiac muscle (also see 8, 11). The possibility, however, cannot be ruled out that cardiac and smooth muscles have functionally equivalent proteins that are distinct either immunologically or in size from skeletal nebulin. An analogous situation was observed for smooth muscles: although low abundance large proteins are detectable on gels (Fig. 2), no proteins that are cross-reactive with either nebulin or titin have been detected (Fig. 3).

Advances in Analysis of Giant Proteins

The analysis of nebulin (and titin) has been facilitated by several technical advances that overcame obstacles confronting earlier investigations. (*a*) Tissue solubilization: direct solubilization of pulverized frozen tissue powder in hot SDS containing protease inhibitors has been successful in minimizing proteolysis. These giant proteins invariably degraded when chunky tissue was added to SDS before heating (unpublished data). (*b*) Size fractionation of SDS-solubilized proteins by NaCl: our serendipitous observation that polypeptide mixture in SDS solution can be precipitated and fractionated by NaCl roughly according to size has been successfully ex-

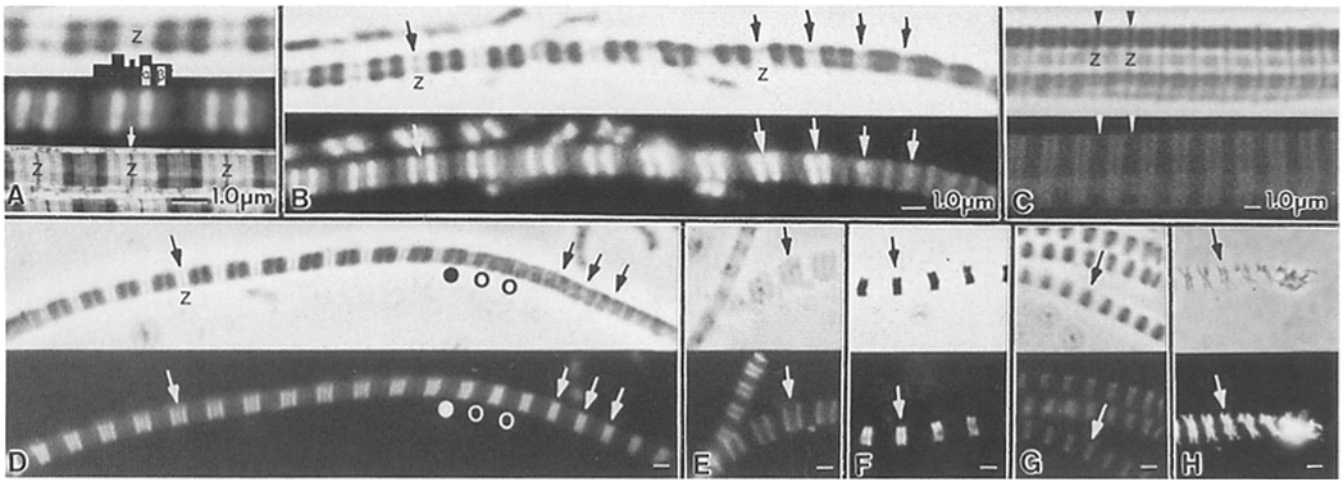

Figure 9. Immunofluorescent localization of nebulin in isolated myofibrils. Rabbit psoas myofibrils, either intact (*A–C*) or previously extracted with 0.6 M KCl (*D–G*) or 0.6 M KI (*H*), were labeled with goat antinebulin and FITC-rabbit anti-goat secondary antibody. (*A*) Typical phase and fluorescence patterns of moderate length sarcomeres are shown (*top* and *middle*); α and β designate a prominent doublet in the I band and a dim zone within the A band respectively. Note that the Z line position is also stained. A low magnification electron micrograph of antinebulin-labeled split fiber is included for comparison (*bottom*). (*B*) Sarcomere length–dependent transition of staining patterns is shown in a myofibril where sarcomere length decreases from left to right: α bands gradually narrowed into one dim band at the Z line and β zones merged into a sharper line at mid A. (*C*) Staining patterns of very short, double overlap sarcomeres. Note that fluorescence coincides with the phase-dense doublet. (*D*) Transition in staining patterns in KCl-extracted sarcomeres. In this myofibril, the right hand sarcomeres starting at the two open circles have been partially extracted by 0.6 M KCl, while those to the left of the solid circles appear intact. Note the narrowing of α–Z triplet into a brighter doublet in the extracted sarcomeres. (*E–G*) Staining patterns of KCl-extracted sarcomeres. Note that fluorescent bands are either of the same width (*E* and *F*) or narrower (*G*) than the phase bands. (*H*) Staining pattern of KI-extracted sarcomeres. The translocated nebulin near the Z position in the KI residue was brightly stained as doublets. Arrows indicate the Z position throughout. Bars: (*D–H*) 1 μm.

plored to purify titin from vertebrates (18, 24) and physarum (6), to remove RNA and DNA from proteins (18), and in the present work, to enrich nebulin for rapid purification. (*c*) Immunoblots: giant proteins are notoriously difficult to transfer to solid support. The gradient slab gels that we have developed now allow high resolution and efficient transfer (16, 31). The immunoblot analysis of nebulin was complicated by the nonimmunological, but highly selective, binding of antibody–enzyme conjugates to nebulin blotted from SDS gels. This problem was overcome by the high salt buffer used in this work or by the use of protein A–based reagents (unpublished data).

Architectural Organization of Nebulin in the Sarcomere: A Set of Discontinuous, Parallel, Inextensible Filaments Anchored at the Z Line

Our localization studies at both light and electron microscopic resolutions clearly indicate that nebulin is an integral component within the skeletal muscle sarcomere that spans a minimum of 1 μm between the Z line and the distal region of thin filaments. The simplest way to interpret this data is to assume that nebulin constitutes a set of discontinuous, parallel, inextensible filaments attached at one end to the Z line, and that the transverse antibody stripes resulted from labeling of epitopes that are aligned axially (Fig. 10). Despite the lack of knowledge of molecular morphology of native nebulin, it is reasonable to expect that such a giant polypeptide must be highly elongated and slender to conceal itself so well within the sarcomere without being recognized in the past by morphological means. (Recall that a 700-kD protein, if globular, is ~11 nm in diameter and would have been easily detected.) It is interesting to note that a 700-kD polypeptide of either α-helix or β-sheet would have a contour length of 0.92 and 2.1 μm, respectively. Such polypeptides, if fairly extended, can easily span the 1 μm minimal distance in the sarcomere. In any case, given the relative abundance (3%) and size (600–800 kD) of nebulin, it can be calculated that there are about three or four nebulin polypeptides per thin filament in the sarcomere. If nebulin indeed constitutes parallel filaments, there would be no more than four nebulin filaments per thin filament and the number will be proportionally less if each nebulin filament comprises more than one polypeptide linked end to end or in parallel.

A Four-filament Sarcomere Model Incorporating Parallel Nebulin and Titin Filaments

The inextensibility of nebulin filaments as reflected by the stretch resistance of nebulin epitopes (Fig. 8), contrasts sharply with the elastic stretch-dependence of the coexisting I band domain of titin filaments (32). These distinct behaviors indicate that nebulin and titin must each represent a separate set of parallel filaments and cannot be serially connected components of the same longitudinal filaments (24–26). While titin filaments extend all the way close to the M line region (12, 32), there is no evidence at present to distinguish whether nebulin filaments are flush with (Fig. 10 *A*) or protrude beyond actin filaments (Fig. 10 *B*). Similarly the possibility that nebulin can be linked to components near the M line cannot be ruled out.

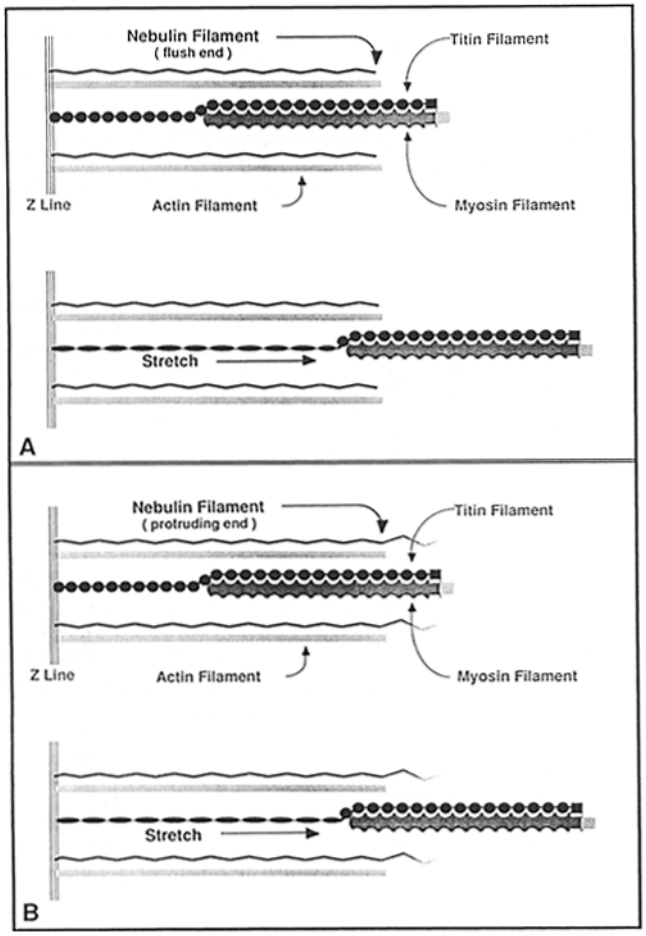

Figure 10. A hypothetical four-filament model of the architectural organization of nebulin and titin in the sarcomere of skeletal muscle. In this model, nebulin constitutes a set of parallel inextensible filaments attached at one end at the Z line. Each nebulin filament represents one, or no more than a few, nebulin polypeptides. Whether nebulin filaments flush with actin filament (*top model*) or extend beyond actin filaments (*bottom model*) is not clear. Titin filaments span from the Z line to the M line region (e.g., the edge of bare zone as depicted here). Each titin filament represents one titin polypeptide. In moderately stretched sarcomeres, only the I band segment of titin responds by extending its length while the nebulin filament, thin filament, thick filament, and A band segment of titin retain constant length. This model ignores the stoichiometry, relative dimension, and lattice spacings of various filaments.

Our data thus suggest that the sarcomere of skeletal muscle may consist of four biochemically distinct filaments–myosin, actin, titin, and nebulin, all of which are directly (actin, titin, and nebulin) or indirectly (myosin via titin) linked to the Z line.

It follows from this model that nebulin filaments, being inextensible, cannot be a primary source of resting tension as recently proposed by Horowitz et al. (7). It is conceivable, however, that nebulin might modulate titin elasticity, if dynamic interactions occur between the two filaments.

N_2 Line and Other Novel Transverse Periodicities in the Sarcomere

The lack of stretch sensitivity of nebulin epitopes and the proposed inextensibility of nebulin filaments raise the question of the molecular composition and structural identity of N_2 lines. Earlier, we have tentatively identified nebulin as an N_2 line–associated protein based on the observation that antinebulin fluorescently stained N_2 lines in the long sarcomeres of glycerinated myofibrils (29). The immunoelectron and immunofluorescence data presented in this paper have persuaded us to abandon this view. We believe that these phase-dense I band striations, which we designated as N_2 lines (29), are artifacts of conventional myofibril preparation that can be eliminated by minimizing proteolysis and mechanical shear during preparation (28). The fluorescent labeling of these N_2 lines by antinebulin and their elastic stretch-dependence as described in our earlier work (29) suggested to us that these striations represent loci on the elastic titin filaments where residual or severed nebulin polypeptides are attached (26). When myofibrils rich in N_2 lines were negatively stained and examined by electron microscopy, massive accumulation of granular material was found at these loci. Such material was absent in sarcomeres without N_2 lines (unpublished data).

We emphasize, however, that the identity and origin of N lines may be far more complex and that it is unlikely that all reported sightings of N lines (i.e., unusual I band striations) can be explained by proteolysis-induced structural changes. For those N line striations that required special treatments to "enhance" their visibility in electron microscopy, such as those described recently by Locker (10), the experimental conditions may have caused the titin/nebulin–containing matrix to undergo an increase in mass density or a change in affinity toward heavy metal ion stains at various loci. This could result from, beside proteolysis-induced translocation, a local shortening of the elastic titin filaments; an interfilament coalescence of a portion of parallel titin, nebulin, and actin filaments; or an enhanced binding of soluble proteins to discreet binding sites on titin and nebulin. For those N lines that were detected as very faint striations in the electron micrographs of rapidly fixed and carefully prepared frog skeletal muscles (3) or for those transverse periodicities that were derived from x-ray diffraction patterns of live frog muscles (2), they may well represent structural features of intact, unaltered sarcomere matrix such as intrinsic variation in filament thickness, extrinsic binding of proteins and ions, or interfilament cross-linking structures.

Thus these uncommon sarcomere striations, being either genuine features or structural derivatives of titin and nebulin sarcomere matrix, are well worth pursuing. In this regard, we suggest that the distinct stretch-sensitivity of titin and nebulin be used as a criterion to classify striations as either "titin-linked" or "nebulin-linked." By this criterion, Cooke's electron dense 230-nm striations in frog muscle (3) may be tentatively classified as partly titin-linked (striations No. 1, 2, 3, and 5) and partly nebulin-linked (striations No. 1 and 4. Fig. 9 C and Fig. 13 of reference 3). (Ambiguity on striation No. 1 exists, since it is very close to the Z line and its stretch response may not clearly manifest until sarcomeres are much longer than those studied by Cooke.) Similarly, the 102-nm transverse periodicity in x-ray diffraction patterns of frog muscles reported by Bordas et al. (2) can be tentatively assigned as nebulin-linked and the 230-nm pseudo lattice as titin-linked. The stretch-dependence of the 230-nm lattice for sarcomeres >2.8 μm has not been demonstrated by the x-ray work.

Is Nebulin an Actin Filament Template or Scaffold?

The architectural characteristics of nebulin (inextensibility, Z linkage, 1 μm minimal length and filament sliding) are highly reminiscent of the behaviors of actin filaments and raise the question whether nebulin and actin are structurally associated in the sarcomere. This question was first raised by us when attempts were made to explain why titin and nebulin filaments were so difficult to identify in intact sarcomeres. We proposed that titin and nebulin might interact with and adhere to myosin and actin, respectively, to form composite filaments, and that these composite filaments may in fact be the morphological structures identified as "thick" and "thin" filaments in electron microscopy (26). The composite nature of titin and myosin filaments is gaining experimental support (e.g., 22, 32); whereas our current data suggest that a nebulin/actin composite filament is worth considering.

This composite filament model has possible implications in the assembly, length regulation, stability, and function of actin filaments. In view of the fact that actin, even in the presence of accessory or capping proteins, is incapable of assembling into filaments of predetermined and uniform length such as those found in skeletal muscle sarcomeres, the idea of a long protein template that directs and regulates assembly of actin becomes increasingly attractive. This idea in turn raises questions regarding the possible participation of nebulin in actin-mediated functions such as actomyosin interaction and its calcium regulation.

Nebulin-free Cardiac Sarcomere and Length Heterogeneity of Actin Filaments

The absence of nebulin in cardiac sarcomeres, though puzzling, offers an unique opportunity to explore the consequence of its absence and to search for useful clues of its function. Although cardiac muscle cells distinguish themselves morphologically from skeletal muscle cells by having highly branched and networked myofibrils, abundant intermediate filaments, and unique junctional complexes at cell borders (19), the fundamental sarcomere architecture has generally been assumed to be identical with each other. A search of literature for more subtle differences revealed that in adult cardiac sarcomeres, not all actin filaments from the same I segment are of the same uniform length (15). This length heterogeneity has been proposed as a structural basis for the unique length–active tension curve that is important for cardiac muscle contraction. We speculate that this heterogeneity may result from the absence of nebulin or a similar protein template which regulates length or stabilizes actin filaments.

We thank Cindy Williamson, Luann Toney, and Gustavo Gutierrez for technical assistance, and Raquelle Keegan for artwork. Drs. Sybyl Street and Roger McCarter instructed us in various single fiber dissection techniques that formed the basis of our split-fiber procedure, for which we are grateful.

This work is supported in part by National Institutes of Health grant DK 20260 to K. Wang who is an Established Investigator of American Heart Association.

Received for publication 4 April 1988, and in revised form 18 July 1988.

References

1. Altman, L. G., B. G. Schneider, and D. S. Papermaster. 1983. Rapid (4 hr) method for embedding tissues in Lowicryl for immunoelectron microscopy. *J. Cell Biol.* 97(5, Pt. 2):309a. (Abstr.)
2. Bordas, J., G. R. Mant, G. P. Diakun, and C. Nave. 1987. X-ray diffraction evidence for the existence of 102.0- and 230.0-nm transverse periodicities in striated muscle. *J. Cell Biol.* 105:1311–1318.
3. Cooke, P. 1985. A periodic cytoskeletal lattice in striated muscle. *Cell Muscle Motil.* 6:287–313.
4. De Mey, J. 1983. The preparation of immunoglobulin gold conjugates and their use as markers for light and electron microscopic immunocytochemistry. *In* Immunohistochemistry. John Wiley Sons, New York. 347–372.
5. Franzini-Armstrong, C. 1970. Details of the I band structure as revealed by the localization of ferritin. *Tissue & Cell.* 2:327–338.
6. Gassner, D., Z. Shraideh, and K. E. Wohlfarth-Botterman. 1985. A giant titin-like protein in physarum polycephalum: evidence for its candidacy as a major component of an elastic cytoskeletal super thin filament lattice. *Eur. J. Cell Biol.* 37:44–62.
7. Horowitz, R., E. S. Kempner, M. E. Bisher, and R. J. Podolsky. 1986. A physiological role for titin and nebulin skeletal muscle. *Nature (Lond.).* 323:160–164.
8. Hu, D. H., S. Kimura, and K. Maruyama. 1986. Sodium dodecyl sulfate gel electrophoretic studies of connectin-like high molecular weight proteins of various types of vertebrate and invertebrate muscles. *J. Biochem. (Tokyo).* 99:1485–1492.
9. Locker, R. H., and N. G. Leet. 1976. Histology of highly stretched beef muscle. IV. Evidence for movement of gap filaments through the Z-line, using the N2-line and M-line as markers. *J. Ultrastruct. Res.* 56:31–38.
10. Locker, R. H., and D. J. C. Wild. 1984. The N-lines of skeletal muscle. *J. Ultrastruct. Res.* 88:207–222.
11. Locker, R. H., and D. J. C. Wild. 1986. A comparative study of high molecular weight proteins in various types of muscle across the animal kingdom. *J. Biochem.* 99:1473–1484.
12. Maruyama, K., S. Kimura, K. Ohashi, and Y. Kuwano. 1981. Connectin, an elastic protein of muscle. Identification of titin and connectin. *J. Biochem. (Tokyo).* 89:701–709.
13. Maruyama, K., T. Yoshioka, H. Higuchi, K. Ohashi, S. Kimura, and R. Natori. 1985. Connectin filaments link thick filaments and Z-lines in frog skeletal muscle as revealed by immunoelectron microscopy. *J. Cell Biol.* 101:2167–2172.
14. Page, S. G. 1968. Fine structure of tortoise skeletal muscle. *J. Physiol. (Lond.).* 197:709–715.
15. Robinson, T. F., and S. Winegrad. 1979. The measurement and dynamic implications of thin filament in heart muscle. *J. Physiol. (Lond.).* 286: 607–619.
16. Somerville, L. L., and K. Wang. 1981. The ultrasensitive silver protein stain also detects nanograms of nucleic acids. *Biochem. Biophys. Res. Commun.* 102:52–58.
17. Somerville, L. L., and K. Wang. 1987. Sarcomere matrix of striated muscle: In vivo phosphorylation of titin and nebulin in frog skeletal muscle. *Biochem. Biophys. Res. Commun.* 147:986–992.
18. Somerville, L. L., and K. Wang. 1988. Sarcomere matrix of striated muscle: in vivo phosphorylation of titin and nebulin in mouse diaphragm muscle. *Arch. Biochem. Biophys.* 262:118–129.
19. Sommer, J. R., and E. A. Johnson. 1979. Ultrastructure of cardiac muscle. *In* Handbook of Physiology: The Cardiovascular system. Vol. 1. R. M. Berne, N. Sperelakis, and S. R. Geiger, editors. American Physiological Society, Bethesda, MD. 113–186.
20. Stedman, H., K. Browning, N. Oliver, M. Oronzi-Scott, K. Fischbeck, S. Sarkar, J. Sylvester, R. Schmickel, and K. Wang. 1988. Nebulin cDNAs detect a 25 kilobase transcript in skeletal muscle and localize to human chromosome two. *Genomics.* 2:1–7.
21. Towbin, H., T. Staehelin, and H. Gordon. 1979. Electrophoretic transfer of proteins from polyacrylamide gels to nitrocellulose sheets: procedure and some applications. *Proc. Natl. Acad. Sci. USA.* 76:4350–4354.
22. Trinick, J. A., P. Knight, and A. Whiting. 1984. Purification and properties of native titin. *J. Mol. Biol.* 180:331–356.
23. Wang, K. 1982. Myofilamentous and myofibrillar connections: role of titin, nebulin and intermediate filaments. *In* Muscle Development: Molecular and Cellular Control. M.L. Pearson and H. E. Epstein, editors. Cold Spring Harbor Laboratory, Cold Spring Harbor, NY. 439–452.
24. Wang, K. 1982. Purification of titin and nebulin. *Methods Enzymol.* 85: 264–274.
25. Wang, K. 1983. Cytoskeletal matrix in striated muscle: the role of titin, nebulin and intermediate filaments. *In* Contractile Mechanisms in Muscle. H. Sugi and H. G. Pollack, editors. Plenum Press, Inc., New York. 285–306.
26. Wang, K. 1985. Sarcomere-associated cytoskeletal lattices in striated muscle. *Cell Muscle Motif.* 6:315–369.
27. Wang, S. M., and M. L. Greaser. 1985. Immunocytochemical studies using a monoclonal antibody to bovine cardiac titin on intact and extracted myofibrils. *J. Muscle Res. Cell Motil.* 6:293–312.
28. Wang, K., and R. Ramirez-Mitchell. 1983. A network of transverse and longitudinal intermediate filaments is associated with sarcomeres of adult vertebrate skeletal muscle. *J. Cell Biol.* 96:562–570.
29. Wang, K., and C. Williamson. 1980. Identification of a N2 line protein of striated muscle. *Proc. Natl. Acad. Sci. USA.* 77:3254–3258.
30. Wang, K., J. Wright, and R. Ramirez-Mitchell. 1984. Architecture of the titin/nebulin containing cytoskeletal lattice of the striated muscle sarco-

mere: evidence of elastic and inelastic domains of the bipolar filaments. *J. Cell Biol.* 99(4, Pt. 2):435a. (Abstr.)
31. Wang, K., B. O. Fanger, C. A. Gayer, and J. V. Stavos. 1988. Electrophoretic transfer of high molecular weight proteins for immunostaining. *In* Methods in Enzymol, Biological Transport. S. Fleishcer, and B. Fleischer, editors. Academic Press Inc., New York. In press.
32. Wang, K., and J. Wright. 1987. Architecture of sarcomere matrix in skeletal muscle-nebulin filament as a thin filament scaffold. *Biophys. J.* 51: 219a. (Abstr.)